An Interim Report

Modular Expansion Joint Noise Mitigation Study

By

Per Reinhall, Jeff Lipton, Waiel Elmadih, Sawyer Thomas

Department of Mechanical Engineering
University of Washington
Seattle, Washington 98195

Prepared for
The State of Washington
Department of Transportation

February 15, 2022

List of contents

List of figures

1. Introduction

Expansion joints are connections in bridges that allow the structure to expand and contract with changing conditions such as temperature, lake level, wind/wave conditions and traffic loads. Allowing this expansion and contraction is necessary to keep the bridge from becoming overstressed and getting damaged.

Several WSDOT bridges – more than 50 state-wide – have the modular expansion joints like those used on the SR 520 bridge. Modular expansion joints are typically used when six inches or greater expansion/contraction is required at a joint. Numerous noise complaints associated with modular bridge expansion joints have been received at bridges throughout the state. Shortly after opening in 2016, WSDOT started receiving noise complaints relating to the large, 16 center beam, expansion joints on the east and west ends. The noise produced by the SR 520 floating bridge is below Federal Highway Administration abatement levels. It should be noted that this bridge uses a next generation quiet pavement system; when tires cross over the modular expansion joints, it produces a change in the dominate sound frequency that stands out from the baseline bridge noise. This study aims to develop a noise mitigation method that reduces environmental noise levels. Environmental noise is well known to decrease the quality of life of those exposed it, so the results from this study can lead to the improvement of the quality of life for residents living in the vicinity of these bridges. The results of this research project can be applied to all existing and future bridges with these types of expansion joints.

Phase 1 of this study examined the noise generation mechanism and its radiation from expansion joints. The objective of this phase 2 study is to develop ways to mitigate the noise as there is no commercially available noise abatement that is cost effective, safe, and durable. The study includes both laboratory and field studies of novel sound mitigation systems to determine their effectiveness, viability, durability, and safety.

1.1. The Modular Expansion Joint

To reduce the noise coming from the SR520 bridge, the general design of the modular expansion joint (MEJ) has to be considered. The expansion joint consists of a closing box connected to a concrete block (one side of the bridge) and an opening box connected to the other side (see Figure 1). A central beam runs between the boxes leaving room towards the end of one box for expansion and contraction[2]. Supported on the central beam are the I-beams which protrude out of the sub-structures of the expansion joint forming a travel surface with the rest of the bridge.
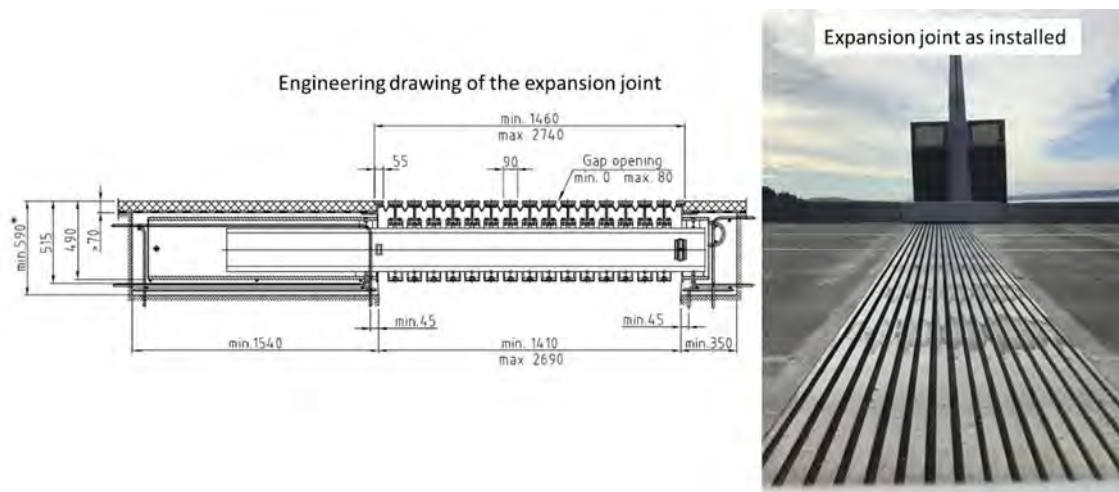
Figure 1. Expansion joint as designed (left) and installed (right). The I-beams run across the lanes to provide a continuous medium of traffic with the two sides of the bridge.

The main material used in the expansion joint is steel with various hardening and grades in some critical regions, for example at the hooks that connect to the concrete. A gap exists between any two I beams (including the edge beam and the first I beam from each side). This gap changes width with the opening and closing of the beams. A seal made of a flexible material (Neoprene) is connected at the opening (below the surface of travel) for collecting debris, dirt, water and/or any parts/particles that can potentially cause damage to the substructure of the expansion joint. A large, enclosed cavity exists underneath the expansion joints of the SR520 bridge. As shown in the Phase 1 report, this cavity is very effective in reducing the noise that radiates downwards from the expansion joint. The cavity also provides easy access to the expansion joints for servicing and replacing parts.

1.2.   *The Source of noise*

The source of the noise was discussed in detailed in our previous research report for Phase 1 of this study that was prepared for WSDOT, January 14, 2019. This report showed that the noise that from the expansion joint are due to:

1) The acoustic resonances of the air cavity enclosed by the tire, seal and the beams.
2) Motion of the beams as they are excited by the tires when they strike the edges of the beams.
3) The vibration of the tires as they strike the beams

Additional conclusions from Phase 1include:

1. The noise as evaluated by the energy spectral density (ESD) at residential locations is highest between 400 Hz and 800 Hz. ESD at the bridge close to the expansion joint is also highest between 400 Hz and 800 Hz.
2. Most of the noise radiates from **the top** of the modular expansion.
3. Frequency characteristics of the noise for vehicle-pass events are closely related to vehicle tire width. The frequency peak for wider tires occurs at lower frequencies than for narrower tires. This is due to excitation of the air volume between the tire and the air gap between center beams.
4. A concrete joint cavity enclosure (WSDOT design) on the SR520 bridge significantly reduces the noise coming from underside of bridge
5. Filling the gaps between the center beams could significantly reduce the noise on the SR520 bridge and other expansion joints.

Understanding the cause of the noise is critical for exploring potential solutions. The previous Phase1 report from the University of Washington (UW) successfully showed the levels of noise at various frequencies. The noise is generated from a range of various sources with a wide range of frequencies (see Figure 1). In this work, we identify three main generation mechanisms. The first one is acoustic radiation from the expansion joint I-beams when the tires hit the edges beams. The dominant frequency in this generation mechanism is the resonance of the I- beams. The second generation mechanism is acoustic radiations from within the cavity formed by the seal,

the tire and two neighbouring I beams. The nature of this acoustic radiation is the air within the cavity and thus the dominant frequency stems from an acoustic resonance. The third mechanism is the vibration of the tires as they are excited by the uneven surface of the expansion joint.

The deformation of the tire and the excitation pressure on the MEJ I-beams as it rolls across the expansion joint are simulated (see Figure 2) with the help of a finite element model[3] of the tire a section of the expansion joint.
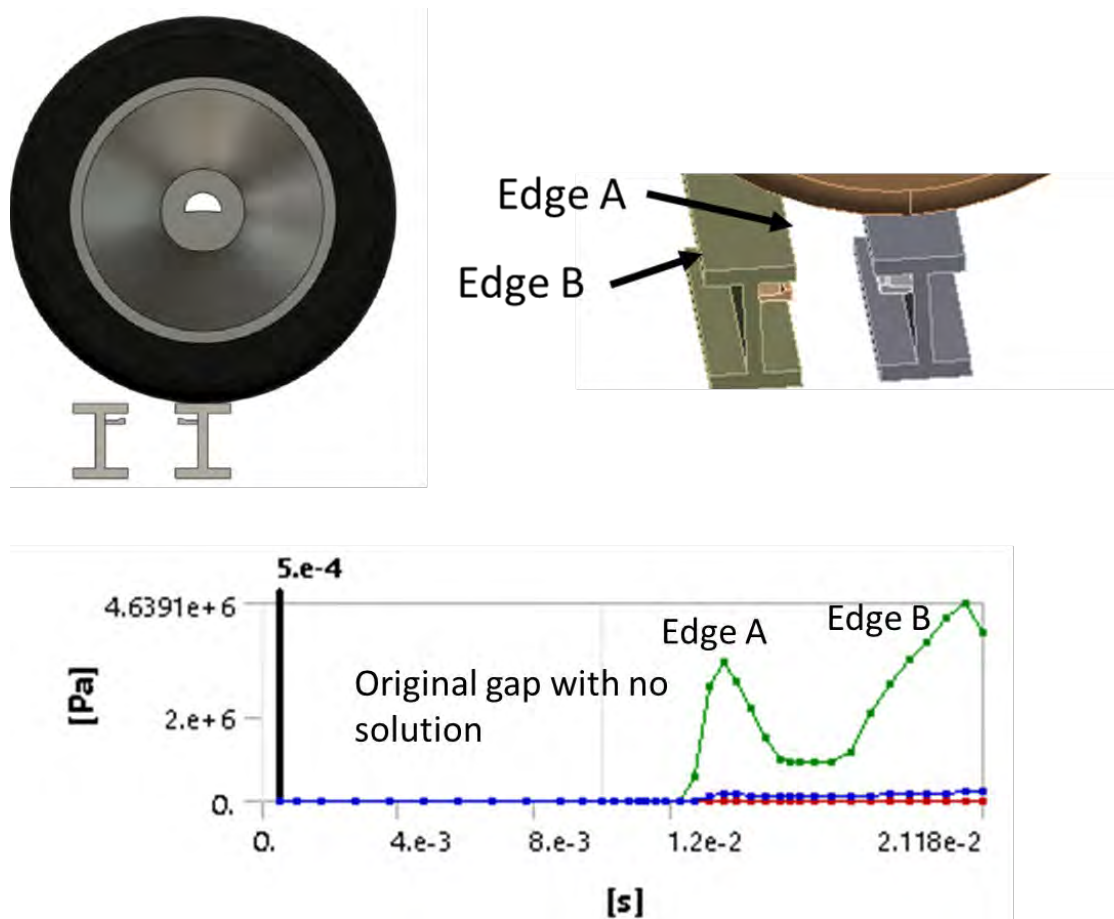

Figure 2. The design of the tire and the I beam. The model sees the tire pushing down on the rail with a force equivalent to that of a typical car (4.47 kN). The tire is driven from left to right at a constant speed of 60 miles per hour and the maximum (green), average (blue) and minimum (red) pressure on the top surface of the I-beam is calculated.

2. Noise Mitigation Design

As described in our previous Phase 1 report it is necessary to address the three noise generation mechanisms in order to create an effective noise mitigation treatment. This can be done by reducing the resonance amplitude of the I-beams as they are impacted by the tire, the acoustic resonance amplitude of the air cavity under the tire, and the noise from the tire as it rolls across the MEJ.

All three noise mechanisms depend on the pressure spikes as the tire rolls across the MEJ. Lower pressure spike will result in less noise generation. A smother surface will result in lower beam vibration amplitude, lower amplitudes of acoustic resonance, and less noise from the tires. Hence, reducing the pressure spikes tackles the main sources of the noise at the same time. One cost effective way to accomplish this is to fill the gap between any two I-beams with a flexible structure. Doing that prevents the free vertical travel of the tire into the gap and hence decrease the pressure spike created when the tire strikes an I-beam after a gap.

2.1. Design Constraints

Geometric and structural constraints of the MEJ create a challenging design problem. First, the structure must allow the MEJ to regularly open and close with gaps that shifts between .84" to 3" during normal operation. Under extreme conditions the MEJ can potentially completely close to 0" gap or expand to a width of 3.85". If the gap fully closes, the design must be easy to remove and in a worst-case scenario, the structure must selectively fail to ensure that no damage occurs to the MEJ or bridge. Second, the support structure must effectively withstand the forces generated by the vehicle tires to significantly reduce noise. Additionally, the solution should also be easy to install, durable and include a moisture seal to prevent dirt, gravel, water, etc, from penetrating the substructure of the expansion joint. These requirements necessitate a unique structure design that must have a horizontal expansion ratio greater than 3.5 while still being able to support the weight of a semi-truck in the vertical direction.

2.2. Multilayer Design Details

To fully support the load of roadway vehicles, we designed a two-layer structure[4] to resist deflection and decrease the impact of the tire on the beams. This design is shown in Figure 3. We

analysed different potential designs using finite element analysis to determine the reaction of the structure under loading of a vehicle's tire. Key metrics for structural design included minimum deflection of the support and minimum resultant pressure on the leading corner of the MEJ beam. Through a long series of design iterations, we have selected two potential solutions for the top support and two potential solutions for the bottom support.
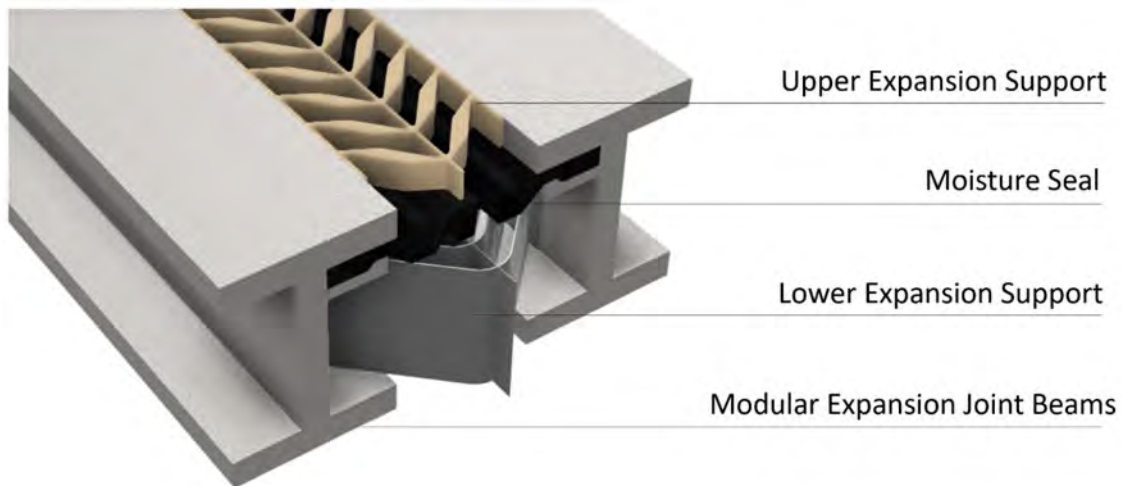
Figure 3. General configuration for the modular expansion joint support structure.

2.2.1. Top support

To offer an effective solution, the top support structure must successfully fill several design requirements. It must be durable enough to withstand roadway abrasion, weathering, and a high number of repeated loading cycles. It must also repeatedly compress and expand between .85" and 3" without undergoing permanent deformation or fatigue. Under extreme compression it must fail and squeeze out of the MEJ without causing any damage, meaning that materials that might damage tires when on the roadway (such as steel) cannot be used. For easy implementation, it must also be simple to fabricate, install and remove.

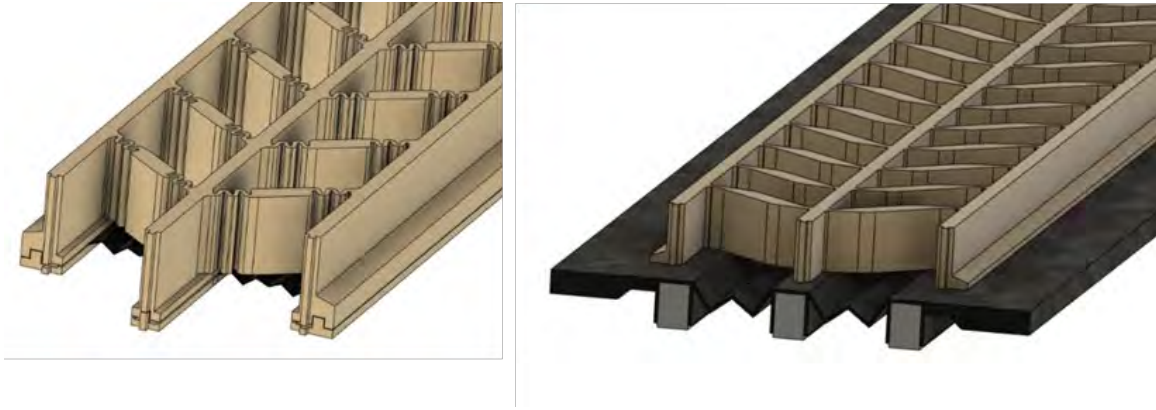Figure 4. Top support structures. (Left) Chevron design features an S-shaped hinge to reduce internal stress. This allows the structure to be fabricated from a stiff material such as PVC. (Right) We fabricate the structure from a flexible material such as neoprene rubber.

Rather than creating a traditional hinge design, which has durability issues and can be susceptible to blocking with grime and binding, we designed chevron structures with compliant flexure joints. We investigated two potential material types with deformable properties, semi-rigid plastic, and, high-durometer rubber. These structures can be easily 3D printed for prototyping or injection moulded for large scale manufacturing. Keyed notches at the front and back of each section allow several short sections to be easily fit and glued together for easy fabrication and implementation. For the rigid plastic version, the moisture seal consists of creased plastic sheeting or extruded rubber and can be connected in the keyed slot shown in Figure 4 (left). For the rubber version, the moisture seal can be made from extruded neoprene and wraps around rigid support bars in the I-beam cavity.

2.2.2. Bottom Support

The bottom support structure rests in the I-beam cavity, supported by the lower flange of each I-beam and has far less challenging design constraints than the upper structure. It must repeatedly expand and compress between 5.875" and 2.875", allowing more space to create a rigid structure. No possibility exists for a fully closed configuration, so spring steel is a viable material option. We designed two different support structures, a high-durometer urethane chevron, and a laser cut

spring steel option. We urethane structure offers far less rigidity but could be injection moulded or extruded for a low-cost solution.
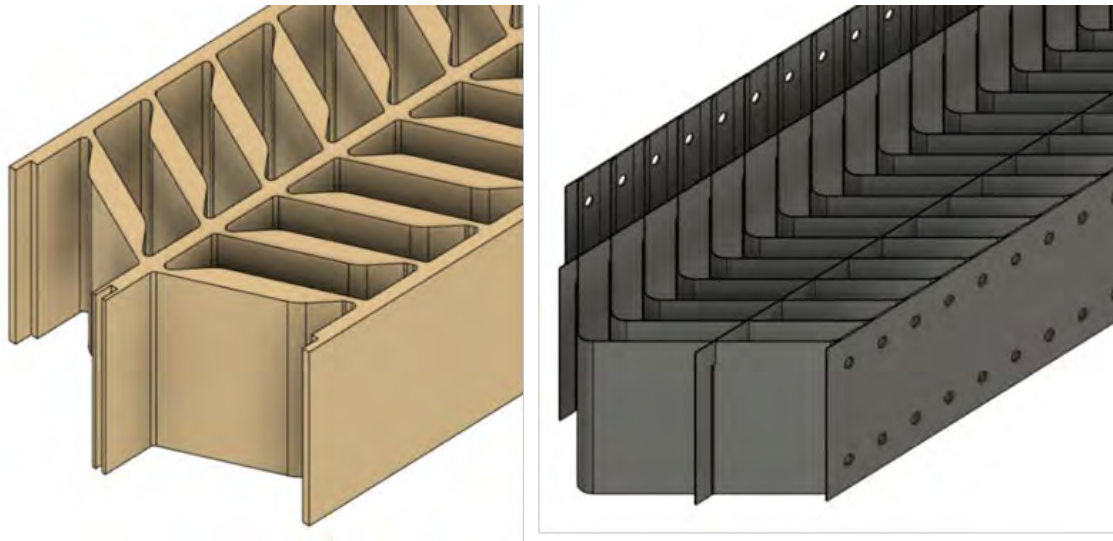

Figure 5. Bottom support structures. (Left) Chevron design fabricated from high durometer urethane. (Right) Structure fabricated from interlocking spring steel.

We fabricated the urethane structure by 3D printed moulds and casting individual chevrons. We then glued overlapping portions to get a single connected structure. The spring steel structure components were laser cut and heat treated to improve elasticity. Notches in each sheet allow easy assembly and chevrons attach to the side plates with bolts or rivets. Both structures can be easily installed by first clamping into a compressed state, zip-tying each section, dropping into the gap, and cutting the zip-ties to expand and secure the structure.

3. Experimental Results

3.1. Compression Testing

To validate our simulations and assess the potential of each design, we built a static compression test setup (shown in Figure 6) with reconfigurable components and tested 8 different configurations for support deformation and edge pressure. We used Fujifilm 70-350 psi prescale pressure paper to determine edge pressure and a IFM diffuse light sensor to measure deformation in the structure. On the physical MEJ, the largest tire deformations and impacts occur when the gap is at its widest point. We positioned the I-beams accordingly to have a 3-inch gap, which is the maximum normal MEJ gap width.
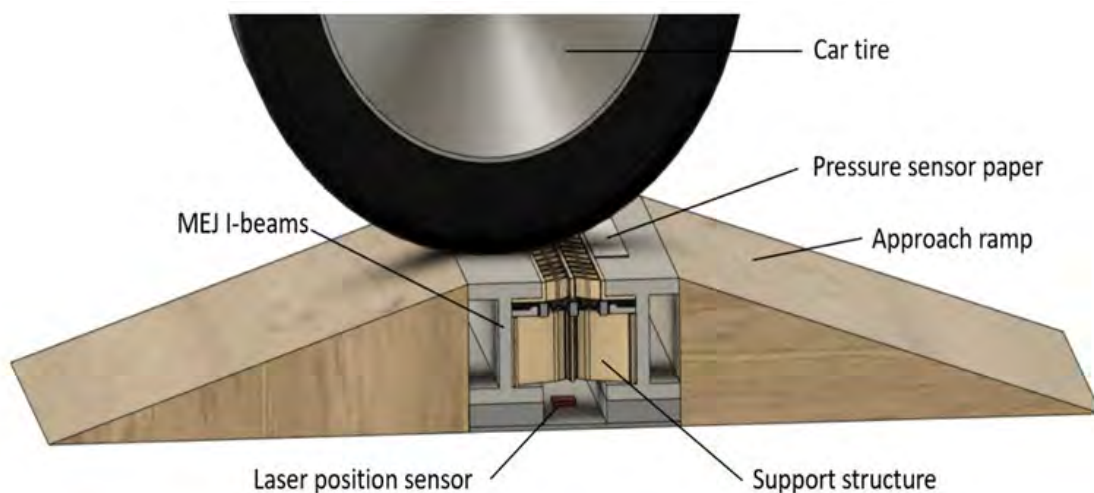
Figure 6. Compression test setup. This test setup matches a two-foot section of the MEJ and can be driven over by a desired vehicle to provide pressure and displacement measurements.

We built the approach ramps from wood and performed our compression tests by driving a Transit Connect van over the setup. Additional variation in vehicle type will be tested to provide a wider range of results. For this specific test, using a single vehicle enabled us to perform side by side comparison of configurations and select the most effective solution.

We tested eight separate configurations (shown in Figure 7) to compare results for each individual support structure and combinations of support structures.
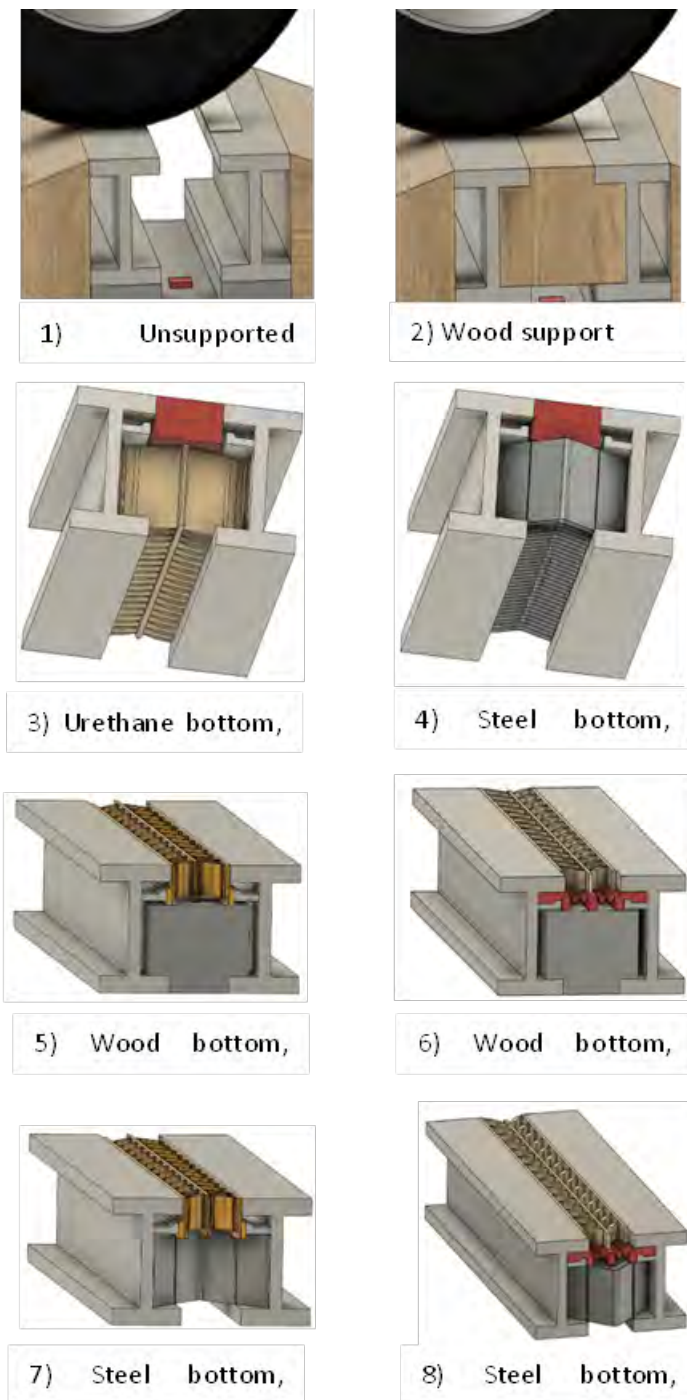

Figure 7. Compression test configurations 1-8. These include baseline testing, individual component testing, and full structure testing.

For baseline testing, we first performed tests with no support structure and a rigid support structure with very little deformation. To create the rigid support, we used layers of ¾" oak planking cut to fill the gap. While this gave a good approximation of a flat surface, some compression still occurred in the wood, particularly at the interface of each rough surface. Next, we tested each of the four support structures individually by combining each with rigid supports as the other section of the structure. Inaccuracies in structure fabrication, dirt, gravel and water on the roadway, and limited sensor accuracy all acted as sources of error in the tests.
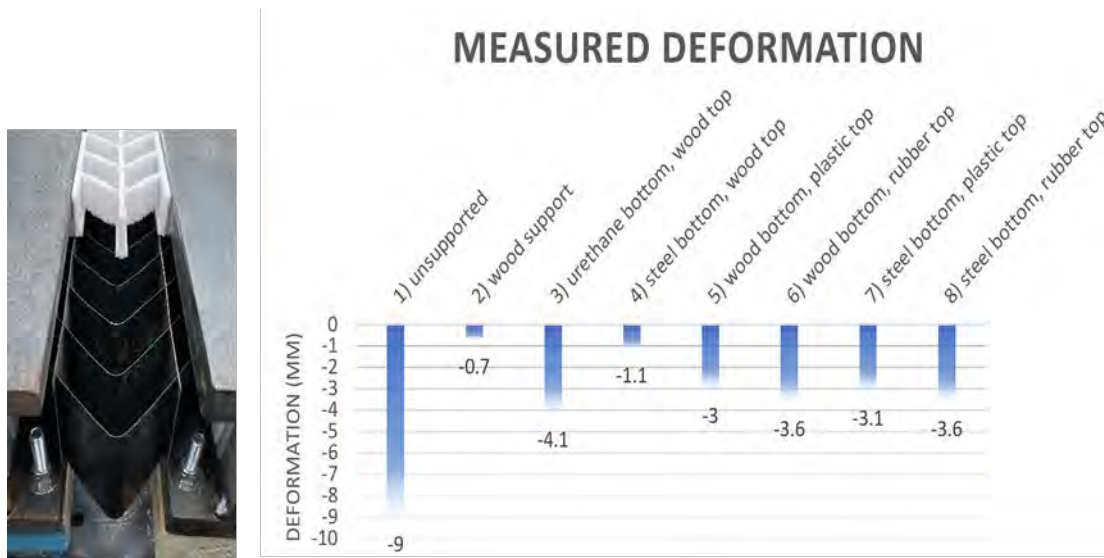

Figure 8. Deformation measurements for each test configuration. Spring steel supported structures greatly reduced tire deformation in the gap. All samples have an error of ±0.4 mm.

To test deformation in the structure, we measured the distance from the lens to a fixed point on the surface of the structure using the diffuse light position sensor and recorded the total displacement as a vehicle drove over the setup. For the unsupported configuration we measured a total displacement of 9mm and for a quasi-rigid support made from oak we recorded a displacement of 0.7mm. Each of the remaining 6 support configurations showed a dramatic reduction in deformation compared to the original gap. The full results are shown in Figure 8. Samples 3, 4, 5, and 6 isolated individual support structures to give an idea of component-by-component rigidity. These tests demonstrated that spring steel lower-support greatly outperformed the urethane lower-support, with a total deformation of only 1.1mm as opposed

14

to 4.1mm for the urethane version. The top supports both had relatively similar deformations, within the margin of error of the position sensor, but the plastic top support demonstrated a slightly lower deformation of 3mm versus 3.6mm for the rubber support. Configurations 7 and 8 tested the deformation of the combined multilayer structure and both provided more than 60% reduction in overall deformation into the gap. Of these options, configuration 7 (spring steel lower support and rigid plastic upper support), offered the most resistance to deformation, showing a 65% reduction vertical of tire displacement. For these reasons we have concluded that the steel bottom will be used in conjunction with either the plastic or rubber top element.

To test the pressure on the leading edge of the I-beam, we used Fujifilm Prescale 70-350 psi pressure sensor paper, which chemically becomes a more vibrant shade of red under direct pressure. This sensing method offers instantaneous feedback and qualitative results but is difficult to quantify with a high level of confidence. We performed post processing on sample images to color code the results. As shown in Figure 9, high pressures (350psi) can be seen as bright orange areas, while low pressures (70psi) show up as dark purple. The support solutions show a dramatic reduction of pressure on the edge of the beam in comparison to the original unsupported sample. Some error can be found in these samples since tiny pressure concentrations such as gravel or misalignment in support height also create small areas of high pressure.
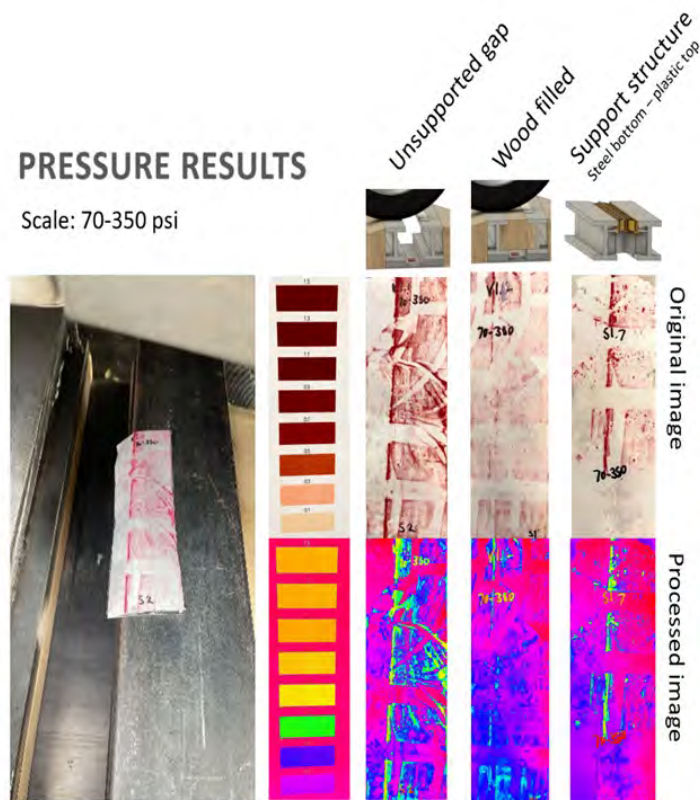
Figure 9. Pressure measurements for each test configuration. All supported configurations have noticeably lower pressure concentrations at the beam edge.

3.2. Simulation Results - Deformation

Simulation of three test configurations (unsupported, rigid support, metal-plastic chevron support structure) are shown in Figure 10. These results show similar trends to our experimental results. Deformation shown in simulation results is much lower than observed in physical tests. Factors that may account for these discrepancies include inconsistent fabrication, compression in rough surface to surface connections, differences in tire size and material properties. All test results indicate a significant reduction in pressure on the beam edges, leading to a reduction in excitation energy and noise. The support structure simulations show a 69% reduction in maximum pressure on the beam and shows only a 30psi pressure increase from the flat, rigid surface simulation.
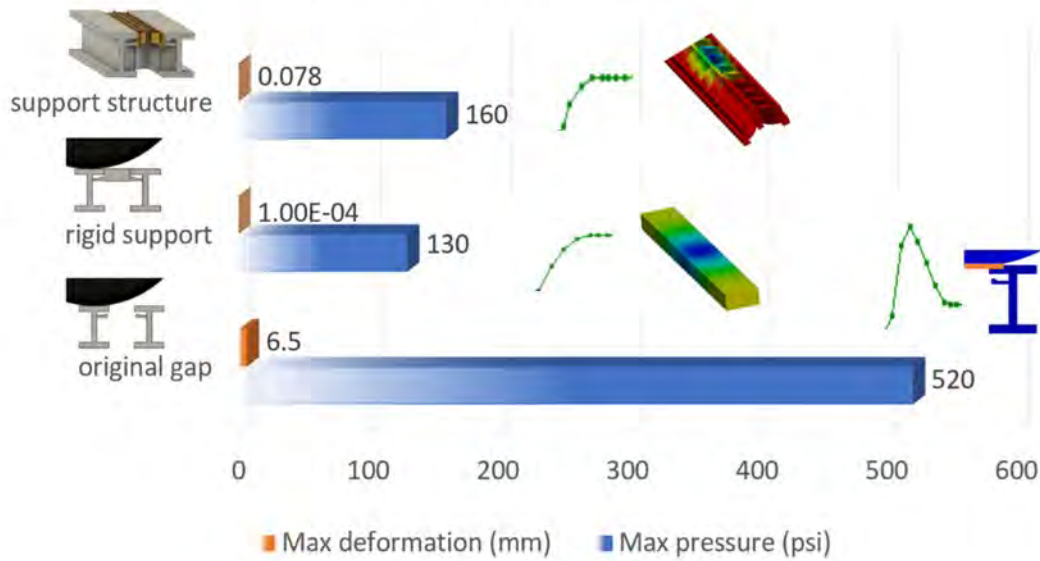
Figure 10. Pressure and deformation results from finite element simulations of each configuration. Icons show the pressure profile as it impacts the beam. The pressure curves show the maximum pressure on the I-beams.

3.3. High Speed Testing

As a car tire rolls over a gap in the road, it impacts the edge of the gap, creating a pressure spike and a resulting noise. To evaluate the acoustic and dynamic effect of top support structures, we are building a high-speed test setup to measure pressure on the beam leading edges and changes in recorded sound. At the widest span, a car tire will only deform roughly 1 cm into the gaps between the beams. This means that we can build a simplified test setup by gluing ¾" steel beams to the roadway and drive over them at 60 mph to get a general comparison of noise with different top supports.
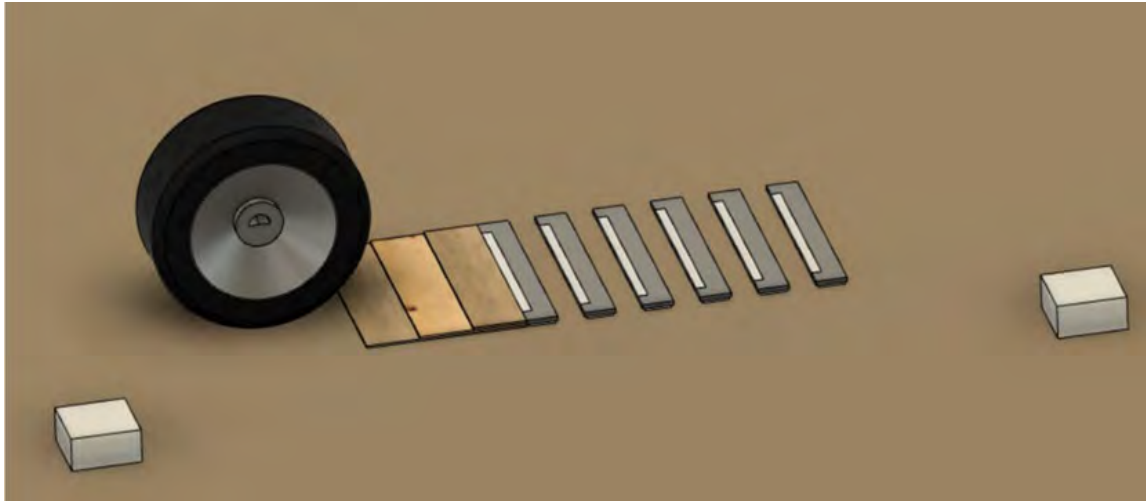
17

Figure 11. High speed test setup. We will roll over 5, 3" gaps made by gluing a wooden ramp and 2'x3.5"x.75" metal beams to the roadway using a silicon-based glue. White boxes represent microphones and white strips on the beams represent pressure sensor paper.

We will measure sound with two microphones positions 10 feet in front of and behind the steel beams. We will measure pressure by attaching Fujifilm Prescale 70-350psi pressure sensing paper to the leading edge of each beam. We will also record tire movement using highspeed videography. We will test three test configurations, unsupported, plastic support, and rubber support. We have ordered all the components to test and hope to run this experiment on Friday 2/18/22.

We anticipate that this will provide us insight into the acoustic response characteristics of the resonances of the top layer structure. This will allow us to determine if the more durable and cheaper to manufacture rubber based top surface will be able to perform comparably to the plastic top surface.

4. Conclusions

A cost-effective noise abatement treatment for modular expansion joints for bridge has been developed. It consists of a flexible two-layer structure that can be inserted between the beams of the modular expansion joint without disassembling the joint (Figure 12). The supporting
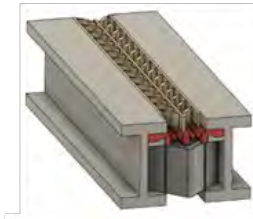

Figure 12. Noise abatement structure for modular expansion joints

bottom layer is a flexible interlocking galvanized spring steel chevron structure and the top structure is a chevron structure with compliant flexure joints made from a mouldable high strength, semi-rigid polymer. The structure has undergone extensive structural analysis, both experimentally and numerically. A high-speed test of the acoustic abatement treatment to evaluate the acoustic performance will be initiated 2/18/22. A full-scale test of the abatement treatment will be performed using one lane of the east modular expansion joint of the SR520 bridge. The exact schedule of this test depends on when we can get access to the expansion joint but we plan to have the experimental plan approved by WSDOT and the fabrication completed by 4/30/22.

References

1.   Spuler, T., Moor, G. & Suilleabhain, C. O. Expansion joints with low noise emission.

2.   Vaitkus, A. & Vorobjovas, V. Traffic / Road Noise Mitigation under Modified Asphalt Pavements Traffic / road noise mitigation under modified asphalt pavements. in *6th Transport Research Arena* (2016). doi:10.1016/j.trpro.2016.05.446

3.   Diggermats UK and Ireland. Ground Pressure. (2021). Available at: https://woodiggermats.azurewebsites.net/ground-pressure/. (Accessed: 1st February 2021)

4.   Wang, N. *et al.* Strain isolation: A simple mechanism for understanding and detecting structures of zero Poisson's ratio. *Phys. status solidi* **251**, 2239–2246 (2014).